THE ASTROPHYSICAL JOURNAL, 384:L53–L57, 1992 January 10

ON THE ORIGIN OF SUBMILLIMETER EMISSION FROM YOUNG STARS IN TAURUS-AURIGA

MARY BARSONY AND SCOTT J. KENYON
Harvard-Smithsonian Center for Astrophysics, 60 Garden Street, Cambridge, MA 02138
Received 1991 September 6; accepted 1991 October 21

ABSTRACT

We present submillimeter photometry of embedded sources in the nearby Taurus-Auriga molecular cloud. We find that, for all sources in our sample, the submillimeter emission contributes 5% or less to the total source luminosity, confirming the relatively "low" luminosity ($0.46\ L_\odot \leq L_\odot \leq 4.2\ L_\odot$) of this class of objects as previously pointed out by Kenyon and coworkers. From the observed 800 μm fluxes, beam-averaged values of the visual extinction are estimated to be in the range $40 < A_V < 500$. However, since all the objects in our sample have 2 μm detections, there must be cavities in the dust envelopes surrounding them. We find that the spectral energy distributions of the embedded sources longward of 300 μm are indistinguishable from those of the brightest, and presumably youngest, of the T Tauri stars, and, furthermore, are uncorrelated with source luminosity, *IRAS* flux, or near-infrared colors. Large submillimeter fluxes, however, do appear correlated with the presence of extended optical and/or near-infrared emission, reminiscent of the recently found correlation between high millimeter flux and the presence of well-developed outflows (Cabrit & André). This correlation suggests the possibility that dust envelope cavities may have been formed by as yet undetected molecular outflows in our embedded source sample.

Subject headings: stars: formation — stars: pre–main-sequence

1. INTRODUCTION

The currently popular picture of star formation (Shu, Adams, & Lizano 1987) outlines an evolutionary scenario consisting of the phases of cloud core formation, dynamical collapse, simultaneous outflow and infall, and, finally, optically revealed star and disk. A series of calculations modeling the spectral energy distributions (SEDs) of young stellar objects (YSOs) resulted in providing a link between this evolutionary scenario and the empirical classification scheme of young stars based on their SEDs (Adams & Shu 1986; Adams, Lada, & Shu 1987, 1988) such that optically invisible sources with steeply rising spectra toward the far-infrared correspond to the dynamical collapse phase and/or the simultaneous infall/outflow phase, and optically visible sources with relatively flat spectra correspond to the optically revealed star/disk system phase.

Newly available submillimeter measurements can provide a test of our current understanding of star formation as well as provide us with new information to constrain future modeling. In this paper we report submillimeter photometry of 10 embedded sources in the nearby Taurus-Auriga molecular cloud, with the goal of improving our understanding of the origin of submillimeter emission from young stars. Section 2 describes our observations, while § 3 presents our results.

2. OBSERVATIONS AND CALIBRATION

We acquired observations of several embedded sources in the Taurus cloud at 1.1 mm, 800 μm, and 450 μm on the nights of 1990 October 28 and 29 with the UKT14 bolometer at the 15 m submillimeter James Clerk Maxwell Telescope (JCMT) on Mauna Kea, Hawaii (Duncan et al. 1990). For a 1 mm column density of water vapor, the filters have effective widths and frequencies of $\Delta\nu = 74.0$ GHz at 271.6 GHz, $\Delta\nu = 101.0$ GHz at 379.5 GHz, and $\Delta\nu = 84.0$ GHz at 676.0 GHz. We collected the data through three different apertures using standard chopping techniques and four integration cycles of 10–20 s each. Table 1 summarizes the aperture sizes and half-power beamwidths (HPBW) for each wavelength.

The output signal from the bolometer, $V_{\rm obs}$, is related to the source flux, $S_{\rm obs}$, by

$$V_{\rm obs} = \left(\frac{S_{\rm obs}}{CK}\right) e^{-\tau A}\ , \qquad (1)$$

where $K = x^2/(1 - e^{-x^2})$ and $x = D/0.6B$. In these expressions, D is the source half-diameter, B is the half-power beamwidth, A is the air mass, τ is the optical depth, and C is the conversion factor between janskys and millivolts. The conversion factor, C, can vary slightly with sky conditions because of the consequent changes in the effective filter bandpasses.

Mars was the primary flux calibrator for these observations. We used the published brightness temperatures of Griffin et al. (1986) and Orton et al. (1986) to determine $S_{\rm obs}$(Mars) for values of K, $V_{\rm obs}$, and A determined at the time of observation. The Caltech Submillimeter Observatory's radiometer measures 1.3 mm optical depth, $\tau_{1.3\ \rm mm}$, as a function of time, and optical depths at our observed frequencies can be determined by using the empirical relationships $\tau_{1.1\ \rm mm} \approx 1.54\tau_{1.3\ \rm mm}$, $\tau_{800\ \mu\rm m} \approx 3\tau_{1.1\ \rm mm} - 3.5\tau_{1.1\ \rm mm}$, and $\tau_{450\ \mu\rm m} \approx 13.5\tau_{1.1\ \rm mm} - 15\tau_{1.1\ \rm mm}$. We measured zenith optical depths in the range $0.04 \leq \tau_{1.3\ \rm mm} \leq 0.07$ for the night of 1990 October 28 and $0.05 \leq \tau_{1.3\ \rm mm} \leq 0.07$ for the night of 1990 October 29. Table 1 lists our derived values for the conversion factor C as a function of aperture size and wavelength. These values remained internally consistent throughout each night's observations. Our photometry for the secondary calibrators OMC-1 and IRC +10216 and the embedded source IRAS 04016+2610 (Ladd et al. 1991a) agrees with previous values.

Mars and the planetary nebula CRL 618 served as pointing calibrators. Typical pointing errors were $\approx 3''$ during the two nights of observation.

TABLE 1

JCMT DATA CALIBRATION

Wavelength/Aperture Size	Date	Conversion Factor (Jy mV^{-1})	HPBW
1.1 mm/65 mm	1990 Oct 28	11.95	18″.5
800 μm/65 mm	1990 Oct 28	9.01	16.8
800 μm/47 mm	1990 Oct 28	13.68	13.5
450 μm/65 mm	1990 Oct 28	20.68	17.5
450 μm/47 mm	1990 Oct 28	22.19	13.5
450 μm/27 mm	1990 Oct 28	28.95	7.5
1.1 mm/65 mm	1990 Oct 28	11.94	18.5
800 μm/65 mm	1990 Oct 29	9.11	16.8
800 μm/47 mm	1990 Oct 29	12.13	13.5
450 μm/47 mm	1990 Oct 29	25.5	13.5
450 μm/27 mm	1990 Oct 29	33.6	7.5

Although the primary goal of our observing program was to acquire single-point photometry for embedded sources in Taurus, we also checked for extended emission by varying the aperture size at a given wavelength. For a point source the measured flux is independent of aperture size, whereas for a source that is extended on the scale of the beam size the measured flux will increase with increasing aperture size (Kraus 1986).

3. RESULTS AND DISCUSSION

3.1. "*Low*" *Luminosities of Embedded Sources in Taurus*

We intended to observe a complete sample of embedded sources in the Taurus-Auriga cloud (Myers et al. 1987; Kenyon et al. 1990), but poor weather limited our coverage to 10 of 15 objects. Table 2 lists submillimeter fluxes and 1 σ errors for these sources, along with average K-magnitudes, *IRAS* luminosities, and submillimeter luminosities. The *IRAS* luminosity, L_{IRAS}, is the 7–135 μm luminosity derived from measurements at 12, 25, 60, and 100 μm (Emerson 1988), while the submillimeter luminosity, $L_{\rm submm}$, is derived with a trapezoidal integration routine from available measurements between 100 μm and 1.3 mm. The submillimeter luminosity, $L_{\rm submm}$, is less than 5% of the total *IRAS* luminosity, L_{IRAS}, for all our sources. Thus, our submillimeter photometry strengthens Kenyon et al.'s (1990) conclusion that deeply embedded sources in the Taurus cloud, as a class, have bolometric luminosities comparable to luminosities of optically visible T Tauri stars.

Assuming a constant star formation rate in Taurus-Auriga over the last few million years, and a typical T Tauri star lifetime of a million years, the ratio of the number of embedded objects to the number of T Tauri stars implies an embedded lifetime of 1.2×10^5 yr in Taurus-Auriga (Kenyon et al. 1990). The embedded phase lifetime is found to be $(3.9 \pm 1.7) \times 10^5$ yr in Ophiuchus (Wilking, Lada, & Young 1989) and 4×10^5 yr or less in the LkHα 101 infrared cluster (Barsony, Schombert, & Kis-Halas 1991).

If most of a star's main-sequence mass is attained in its embedded phase, an accretion luminosity problem arises if one assumes a constant mass accretion rate to stellar dimensions over the embedded phase lifetime. The accretion luminosity, $GM\dot{M}/R$, is 32 $L_\odot$ for $M = 0.5\ M_\odot$, $R = 5\ R_\odot$, and $\dot{M} = 1.0 \times 10^{-5}\ M_\odot\ {\rm yr}^{-1}$. However, the observed luminosities of the embedded objects in Taurus for which we have obtained submillimeter photometry are in the range of $0.46\ L_\odot \leq L_\odot \leq 4.21\ L_\odot$. There are two plausible solutions for this accretion luminosity problem (Kenyon et al. 1990; Beichman, Boulanger, & Moshir 1992): (1) accretion rates during the embedded phase are not constant in time and/or (2) accretion does not take place only to the stellar radius during the embedded phase (viz., the recent calculations of Bodenheimer et al. 1990).

3.2. *Infall Envelopes*

Our data indicate that two of the five embedded sources in Taurus for which we have multiaperture data, 04169+2702 and 04248+2612, are clearly extended on a scale between 13″.5 and 16″.8 at 800 μm, corresponding to $\approx$2000 AU at the 140 pc distance to these sources. Our results for the other three sources are not definitive, although at least one, 04016+2610, is known to be extended at 800 μm from independent measurements (Ladd et al. 1991b). Recent single-dish maps of the submillimeter/millimeter continuum structure of other embedded sources (Chandler et al. 1989; Keene & Masson 1990; Ladd et al. 1991b) show evidence for extended structures on scales of thousands of astronomical units.

The submillimeter fluxes of this sample of embedded sources are indicative of large values of optical extinction (see Table 2). The values of A_V range from 40 to 500 and are probably accurate at the order-of-magnitude level owing to uncertainties in the submillimeter opacity law and the density distribution. The visual extinction, A_V, was derived from $A_V \approx 10^5 \tau_{800\ \mu{\rm m}}$ (Weintraub, Sandell, & Duncan 1991, eq. [27]). We estimated the beam-averaged 800 μm optical depth, $\tau_{800\ \mu{\rm m}}$, from the observed fluxes for a beam size of 1.3×10^{-9} sr and an adopted dust temperature of 35 K. A range in $T_{\rm dust}$ of 20–70 K produces a factor of 5 uncertainty in $\tau_{800\ \mu{\rm m}}$.

TABLE 2

RESULTS

Object	K	F_{100}	L_{IRAS}	$L_{\rm submm}$	F_{450}(65 mm)	F_{800}(47 mm)	F_{800}(65 mm)	F_{1100}(65 mm)	$\tau_{800\ \mu{\rm m}}$	A_V
04016+2610	9.35	55.7	4.13	0.08	3.25 ± 0.46	0.29 ± 0.042	0.31 ± 0.061	0.055 ± 0.016	2.02×10^{-3}	222
04108+2803A	10.36	10.9	0.81	0.03	...	...	0.09 ± 0.030	...	5.87×10^{-4}	64
04108+2803B	10.61	10.9	0.81	0.03	<1.8	0.13 ± 0.030	0.15 ± 0.045	<0.088	9.78×10^{-4}	107
04166+2706	13.70	9.5	0.51	0.03	...	0.63 ± 0.057	0.65 ± 0.035	0.300 ± 0.043	4.24×10^{-3}	466
04169+2702	11.22	16.5	1.31	0.03	...	0.52 ± 0.069	0.73 ± 0.051	0.280 ± 0.025	4.77×10^{-3}	524
04181+2655	10.70	10.0	0.45	<0.02	...	<0.075	...	...	$<4.89 \times 10^{-4}$	<54
04181+2654	10.84	10.0	0.43	<0.02	...	<0.060	...	...	$<3.91 \times 10^{-4}$	<43
04239+2436	8.39	15.9	1.49	0.05	<3.0	0.23 ± 0.025	...	0.077 ± 0.023	1.50×10^{-3}	165
04248+2612	10.68	9.3	0.44	0.02	...	0.12 ± 0.033	0.21 ± 0.039	0.100 ± 0.019	7.82×10^{-4}	86
04325+2402	...	22.4	0.89	<0.05	...	<0.170	...	<0.023	1.11×10^{-3}	122

NOTE.—All fluxes are measured in janskys, and all luminosities are in $L_\odot$ for $d = 160$ pc; $\tau_{800\ \mu{\rm m}}$ was determined using the observed 800 μm fluxes; $d\Omega = 1.3 \times 10^{-9}$ sr; and $T = 35$ K.

Even so, the large near-infrared extinctions implied by these values of A_V, $A_K \sim 4$–50, suggest that many embedded sources should be invisible at K. However, recent near-infrared imaging of embedded objects shows that the majority have extended 2 μm scattered light associated with them (Terebey et al. 1990; Heyer et al. 1990; Tamura et al. 1991). Of the nine objects for which we report submillimeter fluxes, eight have been observed with near-infrared cameras to date. Except for 04108+2803A and 04108+2803B, which are associated with near-infrared point sources, all the embedded sources are associated with extended near-infrared nebulosity on size scales of 2000–10,000 AU. The resolution to this paradox is that the density distribution surrounding these objects must be highly asymmetric even within the infall envelopes.

One obvious way to produce asymmetric infall envelopes is the excavation of the polar regions by a bipolar outflow from the embedded source. Only two of the sources listed in Table 2 have been searched for CO outflows, 04016+2610 (Myers et al. 1988; Terebey, Vogel, & Myers 1989) and 04108+2803B (Terebey et al. 1989). A CO outflow originating from 04016+2610 was detected by both surveys. Although high-velocity CO was not detected from 04108+2803B in the Terebey et al. survey, this nondetection does not rule out the presence of an outflow, since another nondetected object in the survey mode, L1681B, was found to possess an outflow once it was fully mapped.

Although T Tauri stars generally are unresolved in 3″–5″ beams at submillimeter wavelengths (see Adams, Emerson, & Fuller 1990; Evans, Levreault, & Harvey 1986; Sargent & Beckwith 1987, 1989; Weintraub, Sandell, & Duncan 1989), many are associated with extended optical and near-infrared reflection nebulosity. For example, Herbig & Bell (1988) list 22 young stars associated with extended nebulosity, while Tamura et al. (1991) found several near-IR nebulae associated with bright T Tauri stars. These nebulous young stars generally have larger 1 mm fluxes, larger $K-L$ and [25]−[60] color indices, and larger *IRAS* luminosities than young stars without extended nebulae (see Fig. 1). Many of these young stars—particularly those with "flat" spectral energy distributions—also have significant ($p \geq 2\%$) linear polarization at optical and infrared wavelengths (Bastien 1982). The combination of extended nebulosity and large polarization argues for a geometry in which much of the optical/near-IR radiation has been scattered off an extended structure, perhaps an infalling envelope.

3.3. *Correlations*

Figure 1 shows that the 1 mm flux of embedded sources in Taurus-Auriga is not well correlated with the stellar luminosity (L_*), the *IRAS* luminosity (L_{IRAS}), a near-infrared color index ($K-L$), or an *IRAS* color index ([25]−[60]). T Tauri stars in the cloud also show no correlation of 1 mm flux with shorter wavelength emission (Fig. 1). Beckwith et al. (1990) found no correlation between the 1 mm flux and Hα emission for T Tauri stars. The strength of Hα emission generally correlates with optical veiling and [O I] emission in T Tauri stars (Hartigan et al. 1990), so the 1 mm flux does not correlate with these parameters either. The lack of correlations enumerated above underscores the conclusion (André et al. 1990) that a YSO's circumstellar dust structure cannot be determined based on near-infrared data alone.

Figure 2 compares the spectral energy distributions of three embedded sources (*solid curves*) with three of the brightest T Tauri stars (*dashed curves*). The SEDs of the embedded sources

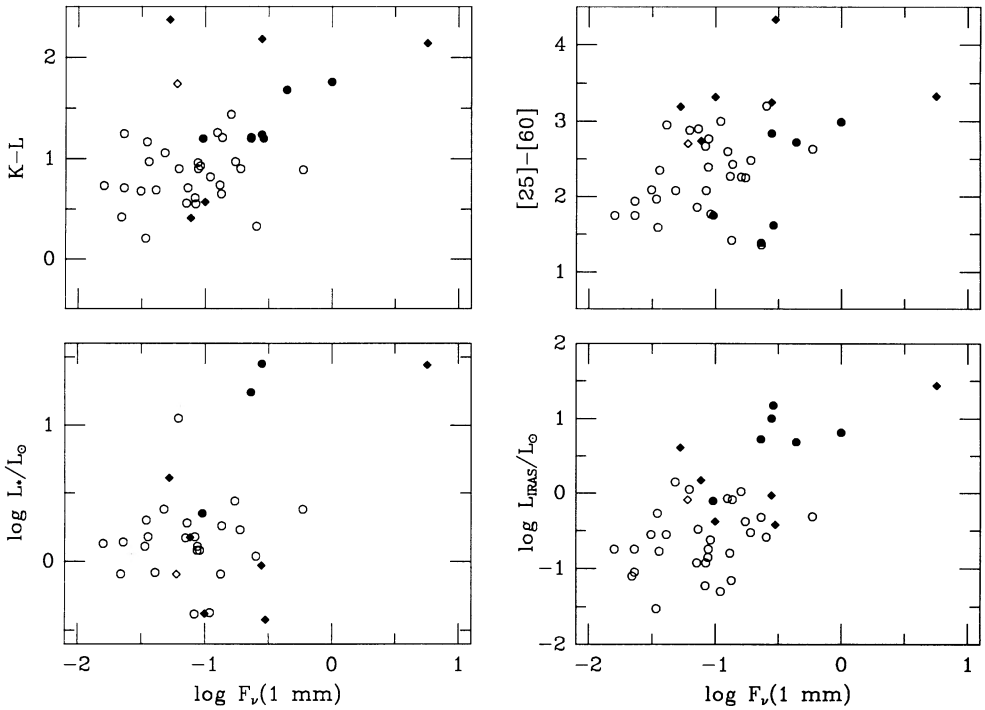

FIG. 1.—Scatter plots of $K-L$, [25] − [60], L_*, and L_{IRAS} vs. 1 mm flux for T Tauri stars (*filled and open circles*) and embedded sources (*filled and open diamonds*). The filled symbols indicate young stars with extended infrared or optical reflection nebulosity. The sources of these data are Adams, Emerson, & Fuller (1990; $F_{1\,mm}$), Beckwith et al. (1990; $F_{1\,mm}$), Cohen, Emerson, & Beichman (1989; L_*), Cohen & Kuhi (1979; L_*), Kenyon & Hartmann (1990; L_*) Kenyon & Hartmann (1992; $K-L$, [25] − [60], and L_{IRAS}), and this paper.

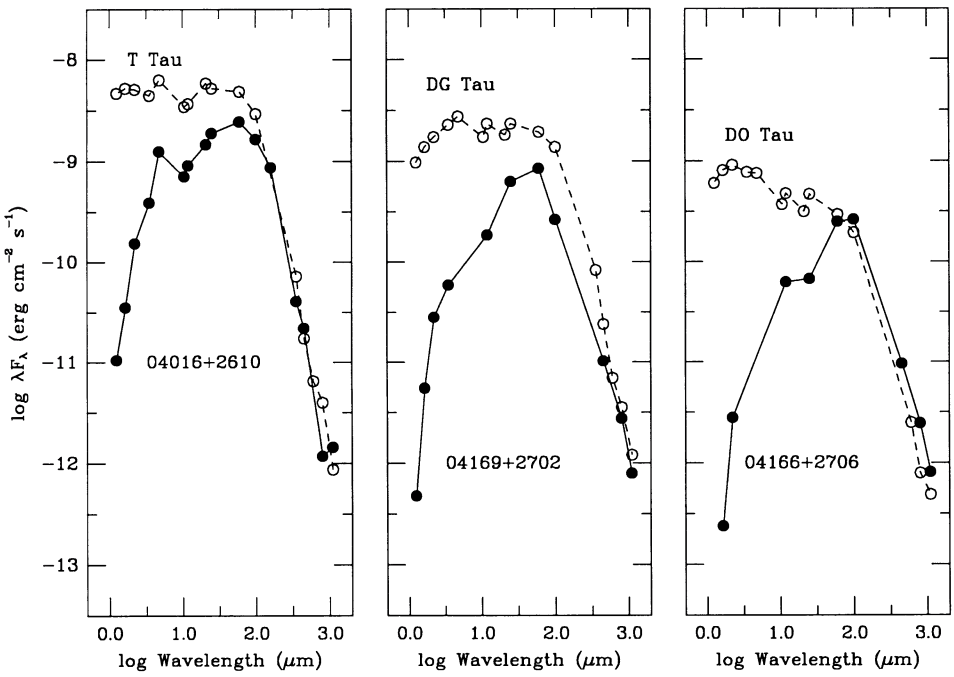

FIG. 2.—Spectral energy distributions for three embedded sources (*filled circles connected by solid lines*) and three T Tauri stars (*open circles connected by dashed lines*). These data have been compiled from Adams, Emerson, & Fuller (1990), Kenyon et al. (1990), Kenyon & Hartmann (1992), Ladd et al. (1991a), Myers et al. (1987), and this paper.

in Taurus-Auriga are indistinguishable from the spectral energy distributions of the brightest T Tauri stars for wavelengths exceeding 300 μm. SEDs for FU Ori objects are also similar to those presented here at long wavelengths (Weintraub et al. 1991). At these submillimeter wavelengths, emission from the outer regions of a circumstellar disk, from an infalling envelope, or from some combination of disk and envelope can account for the slope and magnitude of the SED (Ladd et al. 1991a; Weintraub et al. 1991). Our derived sizes for embedded sources, $R \sim 2500$ AU, suggest that the envelope is responsible for submillimeter emission in protostars (see also Ladd et al. 1991a), and Kenyon & Hartmann (1991) reached similar conclusions for some FU Ori variables.

We suggest that the submillimeter flux from the T Tauri stars plotted in Figure 2 originates from a disrupted, remnant infall envelope. If the envelope covers a fraction f of the sky as seen from the central star, the observed 1 mm flux is then (see Beckwith et al. 1990)

$$F_{1\,\mathrm{mm}} \approx 0.01\ \mathrm{Jy}\, f \left(\frac{\dot{M}}{10^{-5}\ M_\odot\ \mathrm{yr}^{-1}}\right)\left(\frac{r_0}{10\ \mathrm{AU}}\right)^{1.1} \times \left(\frac{T_*}{5000\ \mathrm{K}}\right)\left[\left(\frac{R}{r_0}\right) - 1\right], \quad (2)$$

where $\dot{M}$ is the infall rate, r_0 is the envelope's inner radius, R is the beam radius, and T_* is the effective temperature of the central star. We adopted a 1 mm opacity of 0.02 cm^2 g^{-1}, a beam size of 2″, and a stellar radius of 3 $R_\odot$ to derive equation (2). We expect that most old T Tauri stars will have $f \ll 1$, while younger T Tauri stars with envelope covering factors $f \sim \frac{1}{2}$ can emit $F_{1\,\mathrm{mm}} \sim 0.25$ Jy for $R/r_0 \sim 30$. This idea can be tested with additional higher resolution submillimeter and near-infrared observations of nebulous T Tauri stars. Chen et al.'s (1991) near-IR observations of DG Tau show a 10 AU structure that apparently is not a disk but might be associated with a scattering envelope. If high-resolution observations of other nebulous T Tauri stars show similar structures, then these objects might be evolutionary links between deeply embedded protostars and normal T Tauri stars.

We thank P. André, N. Calvet, L. Hartmann, and B. Whitney for helpful comments on the original manuscript. M. B. extends thanks to C. Chandler and G. Sandell for teaching her use of the JCMT and the intricacies of data calibration in the submillimeter. M. B. was supported by a Smithsonian Postdoctoral Fellowship during the course of this work.

REFERENCES

Adams, F. C., Emerson, J. P., & Fuller, G. A. 1990, ApJ, 357, 606
Adams, F. C., Lada, C. J., & Shu, F. H. 1987, ApJ, 312, 788
———. 1988, ApJ, 326, 825
Adams, F. C., & Shu, F. H. 1986, ApJ, 308, 836
André, Ph., Montmerle, T., Feigelson, E. D., & Steppe, H. 1990, A&A, 240, 321
Barsony, M., Schombert, J. M., & Kis-Halas, K. 1991, ApJ, 379, 221
Bastien, P. 1982, A&AS, 48, 153
Beckwith, S. V. W., Sargent, A. I., Chini, R., & Güsten, R. 1990, AJ, 99, 924
Beichman, C. A., Boulanger, F., & Moshir, M. 1992, ApJ, in press
Bodenheimer, P., Yorke, H. W., Rozyczka, M., & Tohline, J. E. 1990, ApJ, 355, 651
Chandler, C. J., Gear, W. K., Sandell, G., Hayashi, S., Duncan, W. D., Griffin, M. J., & Hazell, A. S. 1989, MNRAS, 243, 330
Chen, W. P., Howell, R. R., Simon, M., & Benson, J. A. 1991, ApJ, submitted
Cohen, M., Emerson, J. P., & Beichman, C. A. 1989, ApJ, 339, 455
Cohen, M., & Kuhi, L. 1979, ApJS, 41, 743
Duncan, W. D., Robson, E. I., Ade, P. A. R., Griffin, M. J., & Sandell, G. 1990, MNRAS, 243, 126

Emerson, J. P. 1988, in Formation and Evolution of Low Mass Stars, ed. A. K. Dupree & M. V. T. V. Lago (Dordrecht: Kluwer), 193
Evans, N. J. II, Levreault, R., & Harvey, P. M. 1986, ApJ, 301, 894
Griffin, M. J., Ade, P. A. R., Orton, G. S., Robson, E. I., Gear, W. K., Nolt, I. G., & Radostitz, J. V. 1986, Icarus, 65, 244
Hartigan, P., Hartmann, L., Kenyon, S. J., Strom, S. E., & Skrutskie, M. F. 1990, ApJ, 354, L25
Herbig, G. H., & Bell, K. R. 1988, Lick Obs. Bull., No. 1111
Heyer, M. H., Ladd, E. F., Myers, P. C., & Campbell, B. 1990, AJ, 99, 1585
Keene, J., & Masson, C. R. 1990, ApJ, 355, 635
Kenyon, S. J., & Hartmann, L. W. 1990, ApJ, 349, 197
———. 1991, ApJ, 383, 664
———. 1992, in preparation
Kenyon, S. J., Hartmann, L. W., Strom, K. M., & Strom, S. E. 1990, AJ, 99, 869
Kraus, J. D. 1986, in Radio Astronomy (2d ed.; Powell: Cygnus-Quasar Books), 3-9
Ladd, E. F., Adams, F. C., Casey, S., Davidson, J. A., Fuller, G. A., Harper, D. A., Myers, P. C., & Padman, R. 1991a, ApJ, 366, 203
Ladd, E. F., Adams, F. C., Casey, S., Davidson, J. A., Fuller, G. A., Harper, D. A., Myers, P. C., & Padman, R. 1991b, ApJ, 382, 555
Myers, P. C., Fuller, G. A., Mathieu, R. D., Beichman, C. A., Benson, P. J., & Schild, R. E. 1987, ApJ, 319, 340
Myers, P. C., Heyer, M., Snell, R. L., & Goldsmith, P. F. 1988, ApJ, 324, 907
Orton, G. S., Griffin, M. J., Ade, P. A. R., Nolt, I. G., Radostitz, J. V., Robson, E. I., & Gear, W. K. 1986, Icarus, 67, 289
Sargent, A. I., & Beckwith, S. V. W. 1987, ApJ, 323, 294
———. 1989, in IAU Colloq. 120, Structure and Dynamics of the Interstellar Medium, ed. G. Tenorio-Tagle, M. Moles, & J. Melnick (Lecture Notes in Physics, Vol. 350; New York: Springer-Verlag), 217
Shu, F., Adams, F. C., & Lizano, S. 1987, ARA&A, 25, 23
Tamura, M., Gatley, I., Waller, W., & Werner, M. W. 1991, ApJ, 374, L25
Terebey, S., Beichman, C. A., Gautier, T. N., & Hester, J. J. 1990, ApJ, 362, L63
Terebey, S., Vogel, S. N., & Myers, P. C. 1989, ApJ, 340, 472
Weintraub, D. A., Sandell, G., & Duncan, W. D. 1989, ApJ, 340, L69
———. 1991, ApJ, 382, 270
Wilking, B. A., Lada, C. J., & Young, E. T. 1989, ApJ, 340, 823